CRTs for ERASME
A detailed review

Abstract

The paper summarizes the difficulties encountered during the last $2\frac{1}{2}$ years with the cathode ray tubes for the precision measuring chain of ERASME, and the measures to overcome them. The specifications of the CRT, now guaranteed by the manufacturer and methods of measuring them are discussed, including an instrument to record spot stability to the order of one micrometer. As the originally selected phosphor had to be replaced, the properties of the new phosphor in comparison with the old one are discussed. The technical and economic consequences of the changeover are considered. Finally, some remarks are made about magnetic screening and the importance of using the optics at the magnification for which it was calculated.

Presented at the Conference on Computer Assisted Scanning Padova,

21st-24th April 1976

* On leave from the University of Stockholm, Sweden.

DD-mb

CONTENTS

1. Introduction

The selection of cathode ray tubes for ERASME was based on 7 years of experience with Ferranti Microspot tubes. During that time these tubes had shown excellent results. (ref. 1). As a matter of fact, it took many years of work to develop the related mechanics and electronics to fully exploit the performance of these tubes (ref. 2). Towards the end of 1972 two ERASME units had been completed, and four more were under construction. At this stage CERN received tubes from Ferranti which exhibited serious faults. This put CERN in a much more difficult situation than other Labs which normally required only one or two tubes. It was not until the Oxford Conference in April 1974 that the problem of obtaining high quality tubes was generally realised and thorough investigations were started by Ferranti into the problems which had arisen with their tubes. At the same time a possible further difficulty arose since Ferranti found that they could no longer obtain sufficiently high quality supplies of phosphor A, and instead proposed phosphor A6 as a replacement.

Several other manufacturers of CRTs were contacted during 1972 and two of them delivered sample tubes. Due to a big effort on Ferranti's part it now appears that all problems with their tubes have been overcome, and they even guarantee their tubes to meet agreed specifications.

Close collaboration with Ferranti was essential during this time, and critical evaluation of the measuring methods and the development of a specific method for measuring spot stability was required. As some laboratories decided to wait until CERN was convinced that the CRTs were again available in good quality, we propose to review the problems and the current situation.

2. Summary of the problems with Ferranti CRTs and modifications introduced to overcome them.

A number of Ferranti CRTs type 75/AFJ delivered to CERN and other laboratories between end 1972 and autumn 1975 suffered from one or more of the following deficiencies.

Bad Spot Quality. Some tubes showed a very peculiar shape of the focussed spot, and spot sizes of more than 40 μm.

Instability of the spot position. The undeflected spot changed its position either suddenly ("jumps") or slowly ("drift"). Typical values of the displacements were 50 to 100 μm but values up to 500 μm were observed.

Catastrophic failures. A few tubes failed suddenly by high voltage break-down through the glass walls.

As mentionned in the introduction it required a considerable effort to find the reasons for the problems with the CRTs and to cure them. The measures which were finally successful are described by Ferranti in Appendix 1.

3. Comparison of CRTs from different manufacturers

In 1972 a number of CRT manufacturers were contacted to find out if they could offer tubes for ERASME. For this purpose a list of tentative specifications was written which was intended as a basis for negotiations. CERN would select the manufacturer who could come nearest to the prescribed specifications, taking into account the price-quality relation. The list of specifications is shown in Appendix 2.

The most important points of this list are:

    spot size
    phosphor spectrum and decay time
    screen noise
    spot stability
    lifetime.

Tube manufacturers normally quote for "typical values". This is not very meaningful when, as in machines like ERASME, the performance depends on the quality of the one tube actually used. Therefore much emphasis was given to achieve guaranteed minimum quality.

Apart from Ferranti there were two firms who offered tubes near to our specifications: Litton and Telefunken.

Litton delivered a sample CRT which had the required performance, apart from high own noise. The phosphor offered was P46 which does not quite fit the characteristics of our objective lens. As will be shown later this could be overcome by an optical filter. However Litton found it difficult to guarantee that future tubes would have the same quality as the sample tube.

Telefunken delivered 2 sample tubes, one equipped with phosphor P11 and the other with P24. The P11 tube had excellent spot size and there was no sign of instabilities. However the P24 did not have acceptable screen quality and Telefunken has not been able to improve this so far.

The following list allows a comparison of the principal properties and test results:

	Litton	Telefunken	Ferranti
Phosphor proposed	P46 P24 possibly	P24	A6 A(P24) possible
Spot size (at half height)	15 μm	20 μm (10 μm measured on P11 screen)	16.5 μm
Phosphor noise	>25%	40% large blemishes	<15%
Stability	good	good	now good
Guaranteed Specifications	No	in principle yes	Yes[1]
Guaranteed lifetime of operation	1000 h	1000 h	5000 h
Shelf lifetime	1 year	1 year	1 year

1) The specifications which Ferranti are willing to guarantee may be found in Appendix 3.

It is obvious that at present the Ferranti tubes are the best choice since the tolerance requirements are met and a guarantee for the specifications is given.

4. The effect of spot instability on the measuring accuracy

To justify the tolerances for spot instability it is useful to demonstrate to what extent a shift of the spot causes measuring errors.

An unavoidable effect of using a flat screen CRT is the pincushion distortion. The non-linearities caused by this effect and due to other reasons are being removed by calibration. This is done by fitting a 5th order polynomial by means of which all measured coordinates can be transformed into an undistorted space. The coefficients of the transformation are valid only for that position on the CRT screen for which they were measured. If this position changes by displacement of the origin new constants are necessary. Using the old constants causes distortions of the measuring results. The size of these errors is demonstrated in Fig. 1. For this figure a calibration was first made under normal conditions. The residual errors were then calculated for the crosses of the calibration grid which were used for the calibration. The residual errors are defined as the difference between the real position of a cross and its position found by the 5th order polynomial. An artificial shift was then introduced by imposing a small offset onto the deflection currents. A new set of residual errors was calculated using the old calibration coefficients but performing a <u>linear</u> fit (magnification, rotation, displacement) to the new position, such as is done for the measurment of pictures using the fiducial marks. The upper line of Fig. 1 shows the histogram of the residual errors. The lower line shows the actual direction and the magnitude of the individual errors. The regular pattern of dots indicates the ideal position of the crosses measured on the calibration grid. The position found by the transformation is marked by the "nodes" of the superimposed "net". The distances between the dots and the "nodes" represent the residual errors.

In the picture 10 µm residual error correspond to the distance between two dots of the regular pattern. The displacement Δ in µm is indicated underneath the photos

For Fig. 1 a shift at 45° was produced. Here the lines linking the "nodes" with each other are curved even in the middle of the picture. As a consequence, straight tracks measured in the centre of the picture would be considered as curved. In the case of 200 µm shift it would cause a sagitta of 10 µm over 10 cm that would be serious for high momentum tracks. Fiducials in the corners of the pictures might be shifted as much as 25 µm.

In Fig. 2 the residual errors are plotted as a function of displacement of the spot. The residual errors after a shift at 90° are plotted in addition to the residual errors found after a shift at 45°.

As a rule of thumb the error which is caused by the shift of the centre can be roughly estimated as follows:

$$E_{max} = \frac{s}{10}$$

$$E_{rms} = E_{av} = \frac{s}{30}$$

where E_{max} is the max. error, E_{rms} is the r.m.s. error, E_{av} is the mean error, and s the shift in μm.

We conclude from the photos and from the plot that for a displacement of the beam of up to 50 μm no appreciable non-linearitics are to be expected.

The simulation of the shift at the deflection coil is the worst case. If the shift were caused by a deflection further away from the screen then the change of the angle of incidence to the screen would be smaller and so would the change of pincushion distortion.

Jumps can be serious if they occur during measurement of tracks or fiducial marks. Long term drifts effectively force frequent calibration of the system. These considerations justify the specification of short term stability (2 μm during 20 min.) and long term stability (50 μm during 24 hours).

5. Method of measuring spot size and stability

Manufacturer and customer must agree about measuring methods and results when specifications of CRTs are to be guaranteed. In the following the two different methods of measuring spot size used by Ferranti and CERN are compared, and a new method of measuring spot stability is described.

5.1 Spot size

2-slit method

At CERN as in most of the similar laboratories the spot size is measured using the 2-slit method. A slit which is small compared to the width of the spot scans over the spot. In this way the intensity profile of the spot is found. A second slit a known distance from the first generates the same profile again. The distance between the two profiles is used to find the width of the profile in absolute terms. The width of the profile at 50% (or 60.6% ∿2σ) is the usual definition of "spot size". For a gaussian curve the conversion between the two width (W) follows the relation:

$$W_{50\%} = 1.18 . W_{2\sigma}$$

Spatial frequency method

Ferranti measures the spot size indirectly by measuring the modulation transfer function (MTF) which is generated by the spot scanning across a bar grid. In this case the spot size is defined indirectly by the number of cycles per cm at which the modulation has fallen to 60% of the low frequency amplitude.

In Fig. 3 typical results of the 2-slit and bar grid MTF methods are shown.

Comparison of the results of the two measuring methods

Fig. 4 shows the bar grid MTF which was calculated from the intensity profile measured with the two slit method. The crosses indicate the MTF measured using the bar grid. It can be seen that the results agree very well. The additional curve of hatched lines marks the MTF which would be generated by a spot having a perfect gaussian profile. This shows that the gaussian curve is a good approximation of the actual intensity profile. On some defective tubes the spot may be surrounded by a "halo". This will certainly be detected on the intensity profile. To show how far this is true in the case of the modulation transfer function a measured intensity profile was modified by "inventing" possible realistic forms of "halo". This was done for Fig. 5. The new profiles were then converted into the modulation transfer functions (Fig. 6). One can see that all assumed halos

deteriorate the MTF by shifting the 60% amplitude towards lower spatial
frequencies. This result suggests that it is safe to specify resolution
at the 60% point of the MTF curve.

Thus it can be concluded that both methods are largely equivalent. For
reference the bar grid MTF curves of some gaussian spots having spot sizes
of sigma between 10 and 25 μm are given in Fig. 7.

5.2 Spot stability

It was found that no manufacturer had the facility to measure spot stability
over long periods with the required accuracy of the ERASME least count of
about 2 μm.

In CRT measuring machines, such as ERASME, instabilities are normally not
detected before the whole measuring chain is assembled and precisely adjusted
following a rather long procedure. As a matter of fact when instabilities are
observed it is not clear if they are due to the CRT or to instabilities of
the mechanic⁻ or the electronic circuits controlling the deflection.

The SST-unit

Therefore an instrument was developed which allows measurement of the CRT
stability separately. It requires only a mechanically stable and vibration
free optical bench, focus and deflection coils, stable electrical supplies,
and a microspot analyzer.

This instrument which is called an SST-unit (Spot Stability Tester) can be
used at the factory or at the laboratory to record the stability of a CRT
over periods of any duration on an strip recorder.

The principle of the measurement is described with reference to Fig. 8. The
SST-unit generates small sweeps in horizontal and vertical directions
alternatively. The spot on the CRT is projected by the objective of the
micro spot analyzer onto a slide which has a square transparent slit on
black background. This projection is aligned such that the horizontal
and vertical sweeps cross the centre of the square. A zero-crossing detector
detects the moment at which the current in the deflection coil passes through
zero. A track detection circuit measures the time between the zero-crossing

signal and the centre of the track pulse generated by the spot crossing the second slit of the square. This time is converted into an analog signal and fed to a strip recorder. The procedure is performed in X and Y alternatively. Any change of the undeflected spot position will change the time between the zero crossing and the track pulse and thus the signals to the strip recorder. The measuring error of the instrument is very small. With a carefully aligned arrangement the drift introduced by the SST-unit itself is smaller than 1 µm in 24 hours. Very fast and short jumps of the spot position would not be seen on the recorder. Therefore an adjustable threshold and a counter are provided to detect and count each jump exceeding a certain amplitude. Further details can be found in ref. 4. In Fig. 9 the output on strip charts of 3 different CRTs is reproduced.

First strip   :   a "jumping" CRT
Second strip :   a "drifting" CRT
Third strip   :   a stable CRT.

6. Properties of phosphors offered as alternatives to the Phosphor A and consequences of their utilisation

In addition to the problems with the CRTs from Ferranti mentionned under 2. Ferranti could no longer supply the originally used phosphor A with the required resolution. As a replacement the phosphor A6 was offered.

Litton supplied a tube with phosphor P 46.

These phosphors A6 and P46 are rather similar in the sense that
- decay time is faster than that of phosphor A: about 0.1 µs instead of 0.5 µs.
- the wavelength of the light is longer.
- the intensity is bigger. P 46 is quoted to be 2 times brighter. A6 was found to be 4 times brighter then A.

The properties of these phosphors will now be discussed in more detail.

6.1 Light emission spectrum

The spectrum of the phosphor must fit to the existing lens, a Zeiss planar f= 300 mm, f: 2.8, 1:0.8. Purchasing of new lenses would require an investment of about 150.000 Sfr. for our 6 machines.

In Fig. 10 the curves of light emission spectra of the phosphors A, A6 and P46 folded with the power sensitivity curve of photomultiplier cathode type S11 are plotted. Above these curves the longitudinal coordinate of the optimum focus of the lens is drawn.

It is interesting to note that the emission spectrum of the phosphor A6 fits even sligthly better to the lens than that of phosphor A for which the lens was calculated. In practice there is however very little difference. If the spot size on the screen is 15 μm, the projected spot is also 15 μm. This applies for the phosphors A and A6. However the the spot of phosphor P46 having also a size of 15 μm on the screen is enlarged to 22 μm. By using an optical filter which cuts the light above 560 nm the spot diameter can be reduced to about 16 μm. The loss of light intensity due to the filter is about 20%. By introducing a high pass filter with cutoff at 455 nm it is in fact even possible to slightly improve the spot size with the phosphor A.

6.2 Comparison between phosphor A and A6

Phosphor A6 is about 4 times brighter than phosphor A, as shown in Fig. 11. This relation is practically constant between cathode currents of 5 and 30 μA. In both cases scanning speeds of 5 m/s and spot sizes of about 17 μm were used.

In Fig. 12 the light output as a function of scanning speed is shown. Again the higher efficiency of phosphor A6 can be seen. It is interesting to note that the highest efficiency is achieved for both phosphors at about 5 to 10 m/s. This is the speed used for measuring in ERASME. There is also a TV-type raster scan which is used for the display of film areas of $2x2 \text{ mm}^2$ to $8x8 \text{ mm}^2$ on a TV screen (Ref. 5). The scanning speeds in this mode are 28 m/s and 110 m/s respectively. The curves in Fig. 12 indicate the reduction of light output from the CRT resulting from the speed increase and the required increase of beam current to compensate for it.

Aging

Fig. 13 shows the result of aging measurements. A stationary spot of 17 µA was used at relatively small currents. The curves agree very well with the formula

$$I = I_o/(1+CN)$$

where I_o = initial intensity, I= aged intensity, C= burn parameter (a constant for a given phosphor) and N= number of electrons deposited per cm^2 (ref. 6). This equation was used to calculate the curves for the normal working current of 20 µA for phosphor A and of 5 µA for phosphor A6 which result in the same light output. For the same light output the life-time of A6 is 3 times longer than of A.

The intensity has fallen to 50% of its original value after 10 minutes in the case of A and after 30 minutes in the case of A6. This time might seem very short but it is in fact quite long. In the case of writing continuously a raster with a repetition rate of 20 Hz, a spot size of 15 µm and a scanning speed of 5 m/s each unit area would be exited during

$$t_E = \frac{15.10^{-6} m}{5 \ m/s} \cdot 20 \ \frac{1}{s} = 60 \ \frac{\mu s}{s}$$

This means each element is only exited during 60 µs per second. A total exitation of 10 minutes = 600 seconds is achieved in

$$t_t = \frac{600 \ s}{60.10^{-6}} \cdot \frac{s}{s} = 10.10^6 \ sec$$
$$\sim 2700 \ hours$$
$$\sim 112 \ days.$$

At higher scanning speeds, and equal beam current and repetition rates, this time becomes proportionally longer. In our system an automatic cut-out assures that a raster is not made over the same area over prolongued periods.

Slow variation of light output of phosphor A6 following a change of
mean incident power

Fig. 14 shows a very peculiar property of phosphor A6. The TV-display was
used for several seconds to scan repetitively an area of $2 \times 2 \ mm^2$ on the
film, and was then switched to a $8 \times 8 \ mm^2$ area such that the area scanned
previously was within the new area. The repetition rate and the beam current
remained the same, but the scanning speed was increased 4 times. Under these
circumstances the previously excited area produced a light output which is
about 50% higher than that from the area more recently excited. This
difference disappears within a few seconds as the light output of the
brighter area decreases and the light output of the less bright area increases.

In Fig. 14 the oscillogram on the left shows the light output shortly after
switching. The higher light output of the previously scanned area is clearly
visible. The two other pictures are taken with a much slower timebase. On
this oscillogram many lines of the TV-raster are written beside each other.
During the first 500 ms the raster was traced on the small area and the light
output was high. At the moment of switching to the large area two levels are
visible. The higher one corresponds to the smaller light output of the newly
addressed area. The lower line corresponds to the light output of the pre-
viously excited area. Both lines move towards each other and join, and after
about 20 seconds the cycle starts again. These pictures suggest that the
phosphor has a higher efficiency when its temperature is higher because on
the small raster the same power is concentrated on a smaller area.

Increase of light output with better focussing

A similar effect is observed when the focus of the spot is changed. The
better the spot is focussed the higher is the total light output. This is
the opposite of what is observed on phosphor A, where the optimum focus is
characterised by a minimum of light output.

Summary of the comparison between phosphors A and A6

	A	A6
light emission spectrum	practically the same	
light output at equal beam current		4 times higher
aging at the same light intensity		3 times longer
screen noise at 15 μm spot width	*)	15%
spot size	*)	15 μm
decay time	0.5 μs	0.1 μs
slow variation of light output	None	**)

*) exact values not known, but at the moment inferior to A6.

**) light output changes over a period of some seconds when the mean incident power is altered. This requires compensation during utilisation.

Conclusion : Phosphor A6 is superior to A at the expense of a compensation for the variation of light output.

7.   Related problems

Two problems were encountered during the measurements of stability and resolution which are worthwhile mentionning: The very great importance of careful magnetic screening and the importance of using the optics only at the magnification for which it was designed.

7.1   Magnetic screening

The tube axis of the ERASME S/M units happens to be perpendicular to the magnetic field of the earth.   This causes a deflection of the non-screened beam of 4.1 mm.   Originally a double μ-metal screen was used which reduces this deflection to 28 μm.   The corresponding screening factor of 145 was considered to be sufficient until it was discovered during our stability tests, that from time to time the spot was displaced by approximately 10 μm. This displacement was caused by switching on and off the magnet of the synchrocyclotron. Which is situated at a distance of about 75 m and produces a change in magnetic field of about 1/3 of the earth's field.   The introduction of a third screening layer and additional shielding in front of the CRT reduced this influence to about 1 μm.

7.2   Utilisation of the objective lens at another magnification.

The Zeiss lens Planar 2.8/300 mm is very carefully optimised for a demagnification of 1 : 0.8.   Fig. 15a shows the resolution at this nominal magnification.   The spot was scanning over a test grid consisting of transparent lines on a black background.   Lines of 25 μm alternate with lines of 10 μm at a distance of 200 μm.   The picture shows the envelopes of the 25 μm and of the 10 μm wide lines.   The resolution is uniform over the whole field of 120 mm.

For Fig. 15b the lens was used at 1:1.   In this case the resolution which is about the same in the centre drops dramatically towards the edges.   The loss is about 2/3 !

In Fig. 15c the lens is used in the reverse sense. It magnifies the spot by 1 : 1 .25 instead of demagnifying it by 1 : 0.8. In this case the overall resolution is much better than the one achieved at a magnification of 1 : 1 in spite of the nominally bigger magnification of the spot.

The test used for Fig. 16 is even more sensitive to deviations from the nominal magnification. In this case a bar grid of 30 μm pitch was used having 200 μm wide reference lines every 10 mm. At 1 : 0.8 the modulation is uniform. At only 5% deviation from the nominal value (1 : 0.75 and 1 : 0.85) the modulation drops visibly towards the edges of the scan. At 1 : 1 there is only modulation in the centre of the field.

8. Acknowledgements

9. Appendix 1 to 3

Investigation and Improvements Incorporated by Ferranti.

by M.R. Bennet

1. Spot drift.

On investigation of several returned CRT's the only
possible explanation of the spot drift was that the beam was seeing
fields introduced from surfaces which were not at a fixed potential
i.e. glass walls of the envelope or insulators holding the gun together.
Two possible places this could happen were between the top of the gun
and the beginning of the graphite wall coating or the gap between the
electrostatic focus lens.

Initially it was decided to stabilise the internal uncoated
wall potential by the application of a conducting coating on the
outside of the CRT which was then held at earth potential. These
CRT's showed some improvements in spot drift but led to a number of
CRT's having their necks punctured due to the high potential gradient.
The results however did show that the hypothesis appeared to be correct.

The next step was to shield both the internal uncoated neck walls
together with a shield to screen the lens gap from both the gun
insulations and the glass walls. The potential of the surface of
these insulators were between 25kV of the final anode and 2kV of the
first anode but any contamination could easily change the surface
potential gradient as could variations of temperature due to self
heating due to the leakage current.

The screening of lens proved to be the most effective change made
on this problem but it was found essential that it was held exactly
coaxial with the lens otherwise the screening electrode itself caused
distortions. In order to maintain this accuracy the general design
of the gun had to be strengthened and this was achieved by adding
many more anchoring points between the various electrodes and the
insulators.

The results of these modifications improved the spot drift to
a few μm over a period of 48 hrs when a number of CRT's were tested

in the Bubble Chamber photograph scanners at CERN.

2. Fuzzy spot.

With a number of the CRT's in question that had been returned, it was found that spots had indeed developed fuzzy edges and when the focusing was removed instead of there being a large clear cut circular spot, it appeared to have curved pieces cut out from the edge. The most usual cause of this was due to charging by secondary emission of insulating layers on beam limiting aperture (BLA) which then deflected the outer edges of the beam. Normally the cleaning process of the gun components precludes this problem. On opening up some of the CRT's it was found that when the getter material (Barium) was being evaporated some of it was getting on the BLA referred to above and it was then assumed that this was becoming oxidised during life and formed the damaging insulating layer.

To avoid this, on the test vehicle CRT's, the getter was initially moved from this position and as an extra precaution the BLA was to be made of a material which either did not readily oxidise (gold, graphite) or if oxidised were of a low resistance (silver).

Various trials were carried out of the above and it was found that, if in addition, the type of getter was changed to the nitrogen doped variety it could be returned to its original position; there being negligible getter material deposited back onto the BLA. This combination of techniques has cured this problem.

3. Triangular spot.

This problem was left to last and fortuitously this problem disappeared with the introduction of the lens screening electrode. It is now obvious that the electrostatic fields from the insulator potentials causing the drift also were the cause of the triangular spots there being 3 rods in a triangular configuration.

APPENDIX 2

Tentative Specifications of the CRT of ERASME

1. Min. useful screen diameter 160 mm.

2. Faceplate: optically flat: thickness 10 mm, parallel tolerance 0.05 mm.

3. Length 750 $\pm$ 5 mm: min. distance between focus and deflection coil 130 mm.

4. The tube should fit without major modifications into the existing mount. Please refer to drawing no. 1244, DD.

5. Max. spot size at the centre of the CRT: 15 μm, measured at a light intensity of about 5 μW/stearadian, and at a scanning speed of 5 m/s. The spot size is defined as the diameter of the intensity distribution curve at 50% amplitude.

6. Phosphor similar to P 24 (please indicate spectrum and decay time).

7. Screen noise <10%, at the quoted spot size and the measuring conditions specified under 5.

8. Few blemishes (specified maximum number and size).

9. Non-deflected unfocussed spot position max.6 mm off the geometrical centre of the tube, magnetic shielding applied.

10. The non-deflected unfocussed spot position must remain within 2 μm during 20 min and not change by more than 50 μm within 24 hours. These values must be achieved after 2 hours running time, all supply voltages well stabilized and constant temperature. This must also be true if the beam current is blanked for prolonged periods.

11. Guaranteed minimum lifetime.

APPENDIX 3

Ferranti have engaged themselves to guarantee to CERN all points of the list of specifications reproduced in Appendix 2 with the following provisos:

to point 5. Spatial frequency

minimum 280 c/cm at 60% MTF. (~16.5 μm at 50%)

to point 6. Phosphor A6. It is possible to deliver phosphor A, but with lower quality at present.

to point 7. Screen noise 15% up to a resolution of 260 c/cm. Above 260 c/cm the noise is allowed to increase linearly to reach 30% at 400 c/cm (~11.5 μm at 50%).

to point 10. The guarantee of stability is subject to availability of the necessary equipment to carry out tests, i.e. of a copy of CERN's SST-unit.

to point 11. Shelf life 1 year with cathode reforming to be carried out as necessary to obtain required emission.
Life time: 5000 hours of operation (heater switched on). The end of the lifetime is defined as a drop of cathode efficiency in the following way:

A quality factor is defined as

$$\emptyset = I_k \ \frac{V_{co}^2}{V_D^{\frac{7}{2}}}$$

where I_k = cathode current
V_{co} = cutoff voltage
V_D = drive voltage (voltage above cutoff)

The end of the lifetime is achieved when $\emptyset$ has fallen to 1.75, a new cathode having typically $\emptyset$=2.9 to 3.0.

10. References

1. H. Anders et al.:   LUCY, a CRT film measuring device - a brief description of the prototype and results of detailed hardware performance measurements.   Proc. Intern. Conf. on Data Handling Syst. in High-Energy Physics, Cambridge 1970.

2. J.C. Gouache: Description and status report of the ERASME system. Oxford Conference on computer scanning. (1974)

3. H. Drevermann: Status of the ERASME system. Padova conference on computer assisted scanning.   April 1976.

4. H. Anders, R.E.S. Berglund: SST, a device to test the stability of the spot position on a microspot CRT.   CERN/ DD 76/8/CERN/EF/INSTR.76-3

5. J.C. Wolles: Description du Système Télévision.   CERN/ERASME note 75-31 Octobre 1975.   CERN DD/EF report under preparation.

6. A. Pfahnl: Properties of fast decay cathod-ray tube phosphors. Bell syst. techn. journal. January 1963.

11. Figure Captions

Fig. 1. Residual errors caused by a shift of the origin in the vertical direction by Δ in μm.

Fig. 2. Plot of residual errors after shifts at 90° and 45°.

Fig. 3. Measurement of spot size:
   a. Intensity profile from 2-slit method
   b. bar grid modulation transfer function (MTF).

Fig. 4. Bar grid MTF of a CRT:
   contineous line : calculated from measured intensity profile
   crosses: measured values using bar grid
   dotted line: calculated using an ideal gaussian intensity profile.

Fig. 5. Intensity profile of a spot with an artificial halo.

Fig. 6. Bar grid MTF calculated from the profiles of Fig. 5.

Fig. 7. Calculated bar grid MTF assuming a perfect gaussian spot of 2σ from 10 μm to 25 μm in steps of 3 μm.

Fig. 8. Principle of the SST measurement.

Fig. 9. Results of SST- measurements
   a. "Jumping" spot
   b. "Drifting" spot
   c. "Stable" spot.

Fig. 10. Light emission spectrum of phosphors P 46, A, A6 and lens correction.
   Lower curves: Emission power spectrum of the phosphors folded with spectral sensitivity of PM cathode S 11.
   Upper curve: Longitudinal coordinate of optimum focus of the lens.

Fig. 11.   Light output of phosphors A and A6 as a function of cathode current at 5 m/s.

Fig. 12.   Light output of phosphors A and A6 as a function of spot speed. The spot scans over a 3 μm wide slit. The peak value of the resulting pulse is plotted. The spot size was 17 μm in both cases.

Fig. 13.   Aging of phosphors A and A6. Light output as a function of time using a stationary focussed spot.

Fig. 14.   Variation of light output of phosphor A6 following a change of mean incident power.

Left: single line taken shortly after switching from small to large area. The previously addressed area is 50% brighter.

Right: many lines written beside each other showing the variation of intensity after switching from a large to small area and back.

Fig. 15.   Loss of resolution when the lens is used for other magnifications than it was optimised for . At 1:1 (20% from nominal value) the modulation drops to 30% in the edges of the field.

Test pattern: 10 μm and 25 μm transparent lines at 200 μm distance on black background. 100% reference bar in the centre.

Fig. 16.   As Fig. 15 but using 15 μm/15 μm bar grid. Steps of 5% change of magnification.

Δ = 200

Δ = 110

Δ = 60

Δ = 0
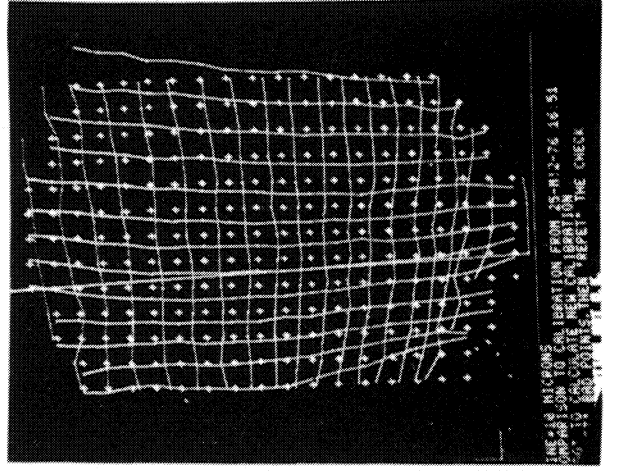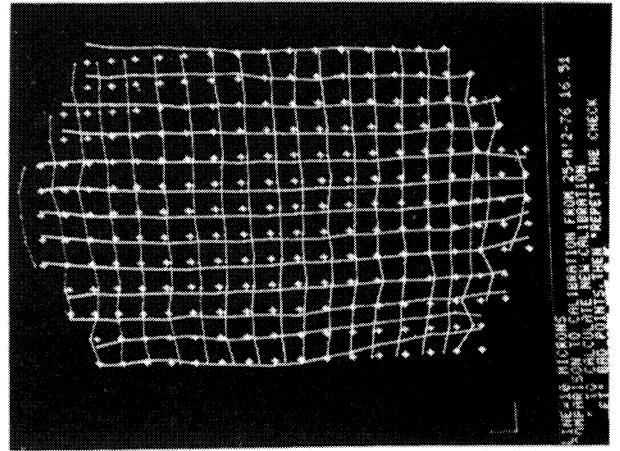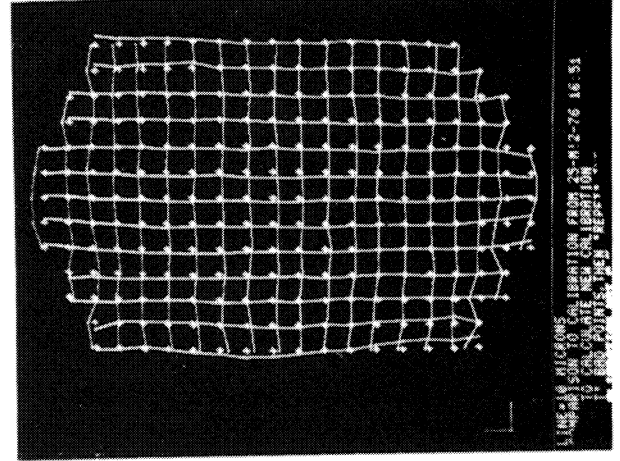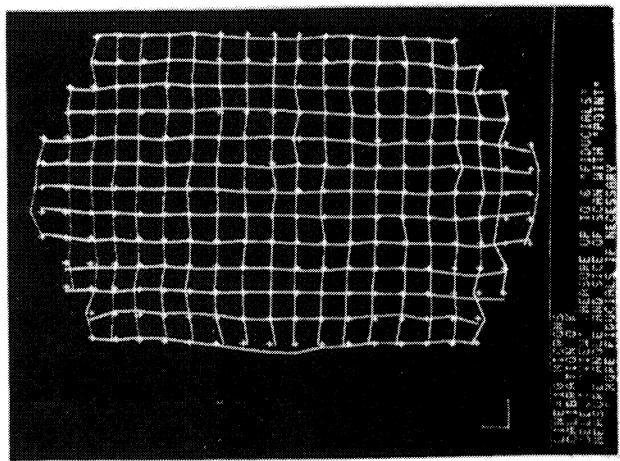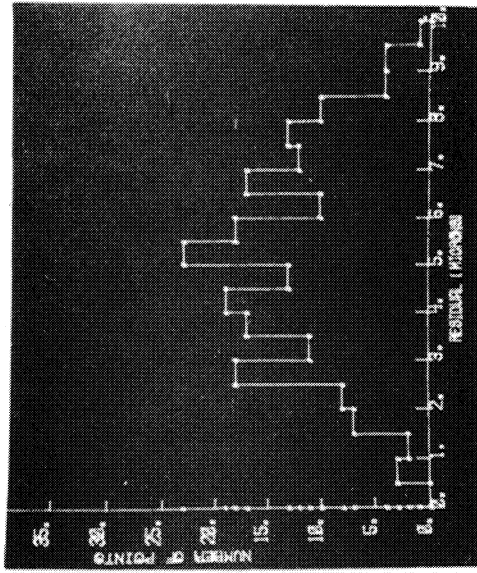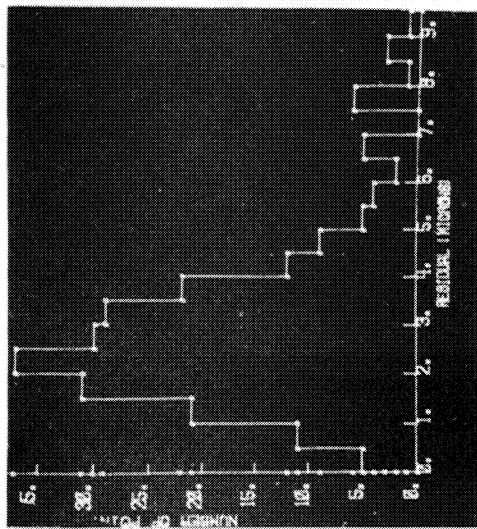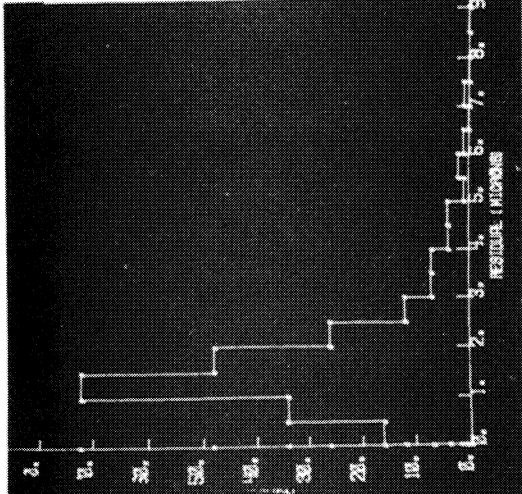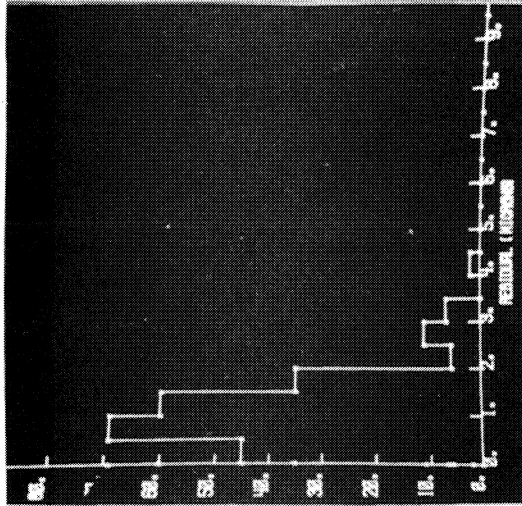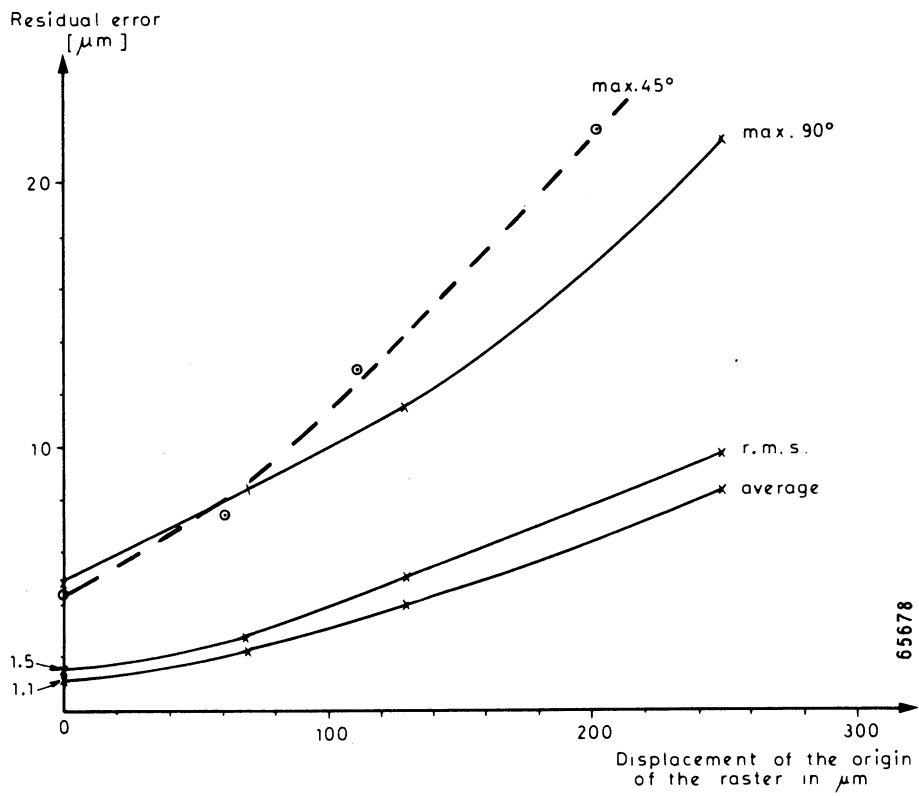
Fig. 1

Fig. 2
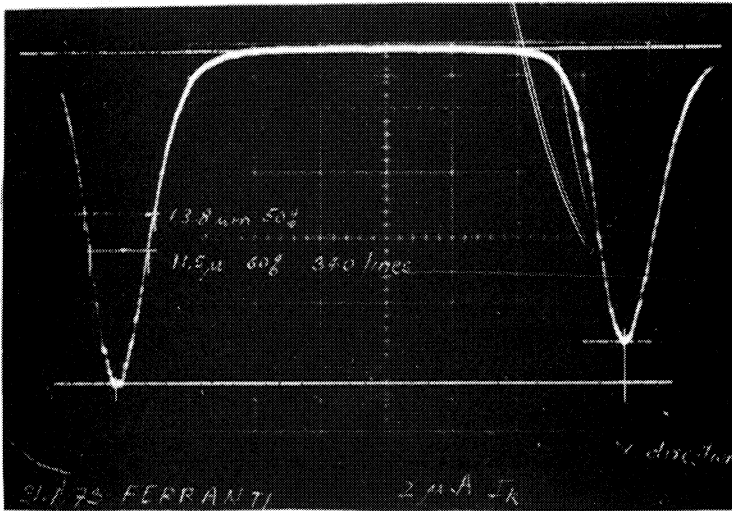
CRT : BO 158

a
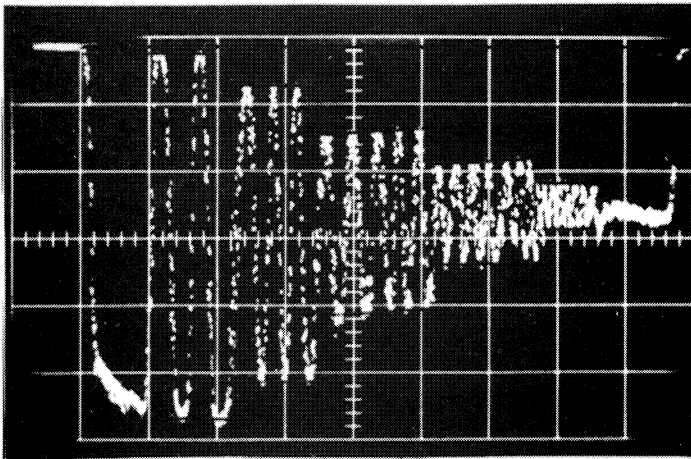
CRT: RI 630

65685

b

Fig. 3

Fig. 4

1) B0158

⊗ measured values

BAR GRID MODULATION (PCT) ABCDEFGHIJKLMN

SPATIAL FREQ. (LINE PR/CM)

65686

Fig. 5

amplitude arb. units

half width in μm

100 %

1 (measured intensity distribution)

60 %

50 %

2
3
4 } "invented" halo

65688

Fig. 6

GAUSSIANS, 2RHO=10.40 STEP 3

BAR GRID MODULATION (PCT) ABCDEFGHIJKLMN

$2\rho = 10\mu m$

65697

SPATIAL FREQ. (LINE PR/CM)

Fig. 7

250 μm

10 μm

SPOT
$\phi \approx 20 \mu m$
SPEED
$0,5 \mu/\mu s$

Z - CROSSING
DETECTOR

VIDEO
SIGNAL

OSCILLATOR
ENABLE

0,5 Mhz   0,25 Mhz

65690
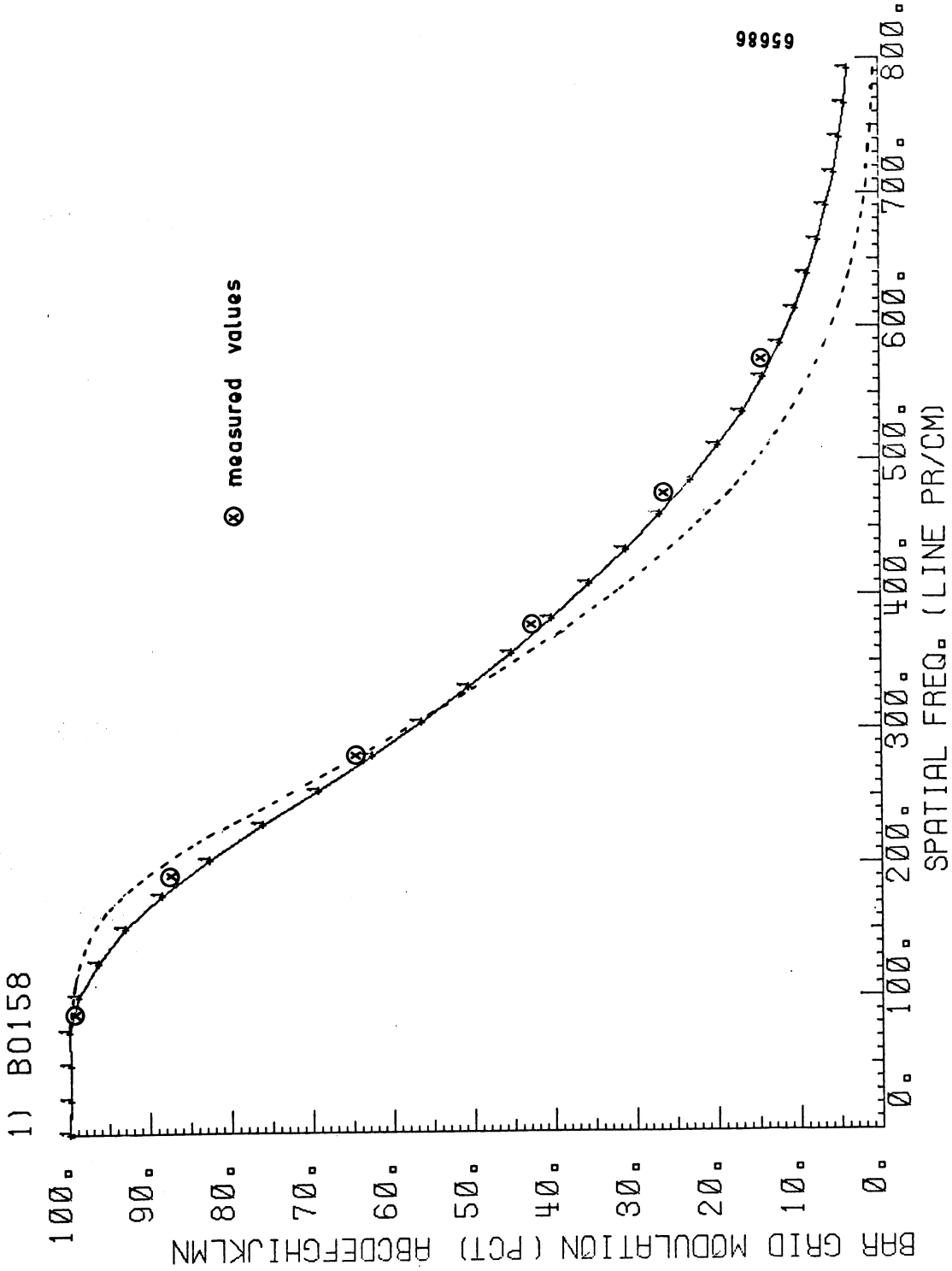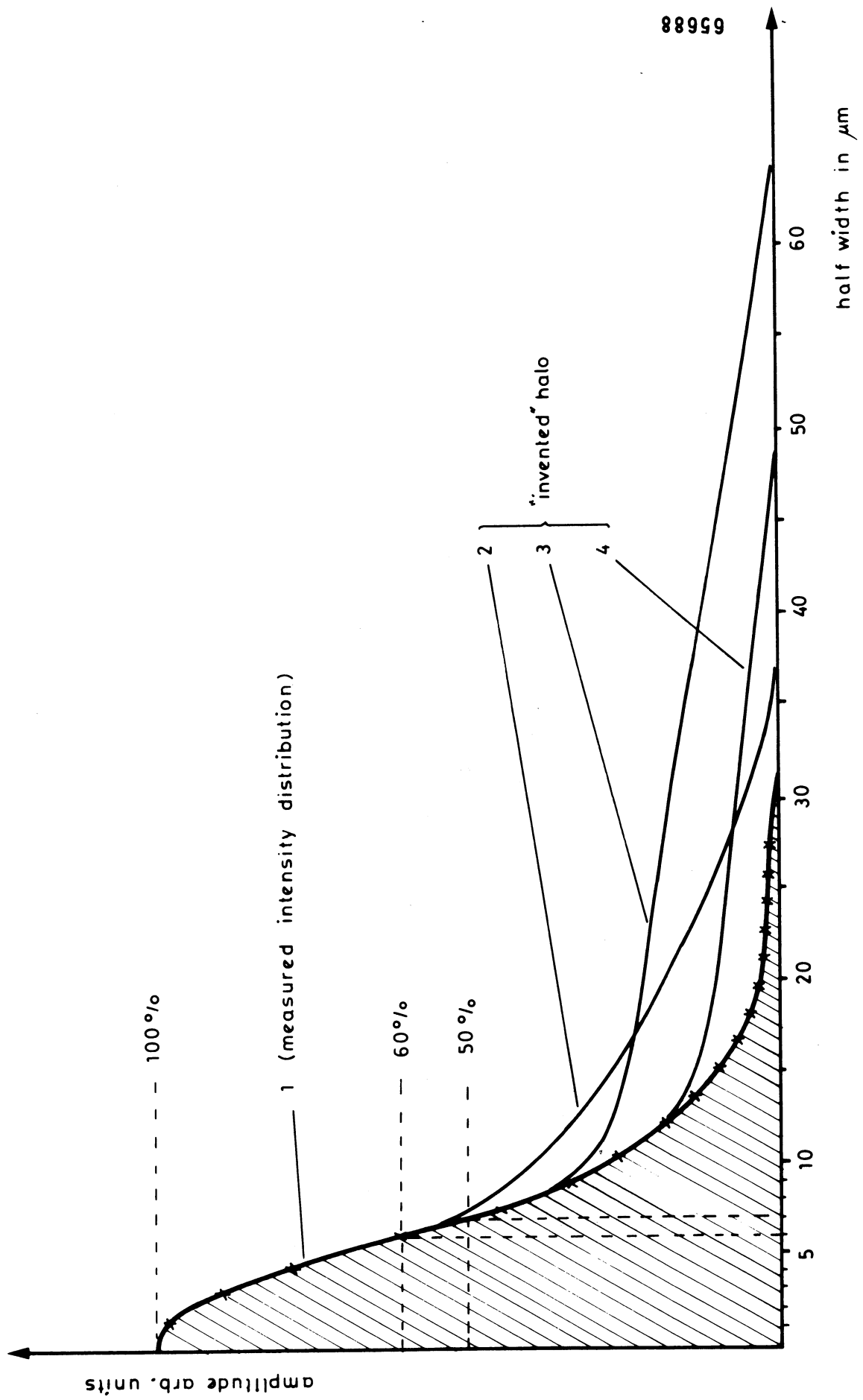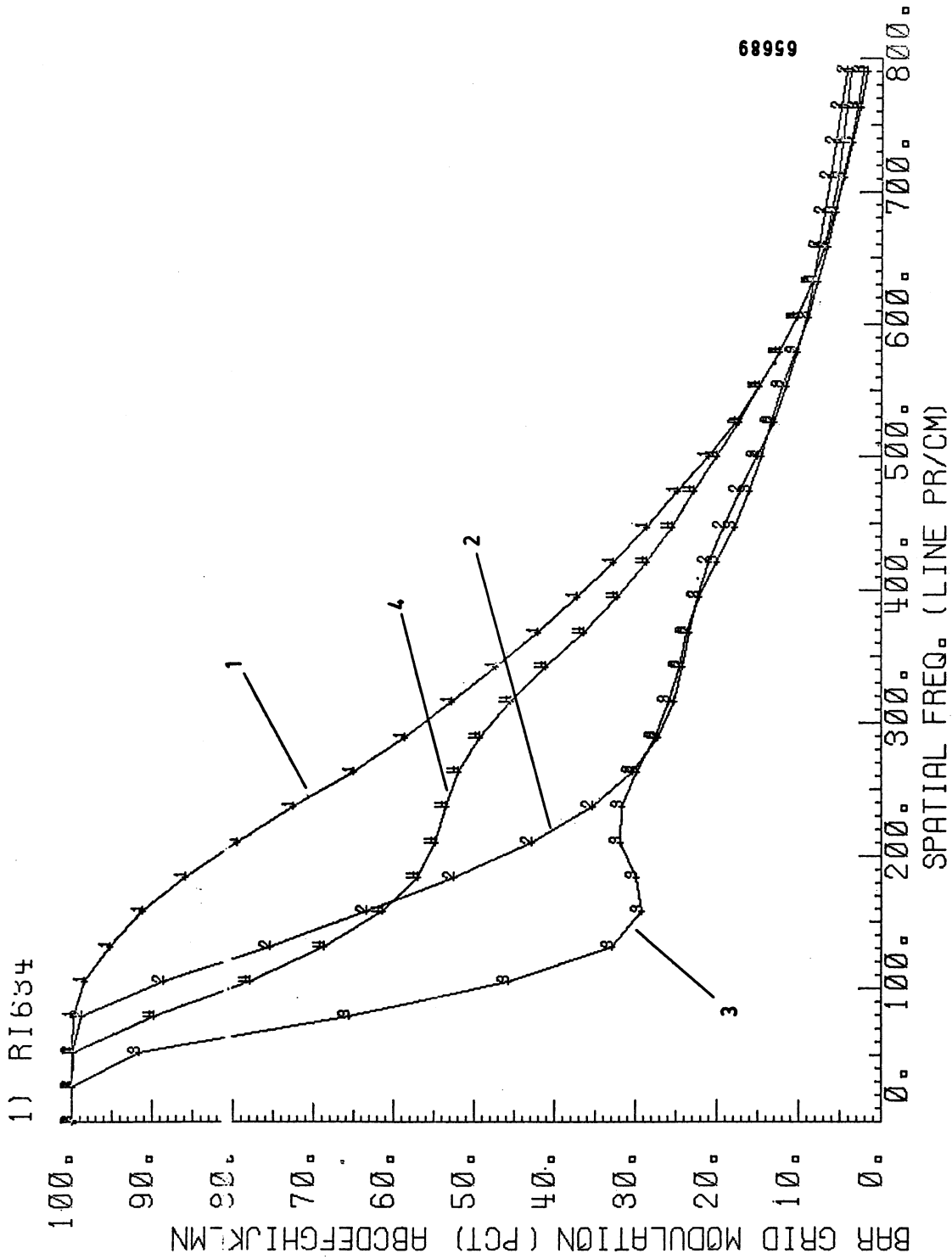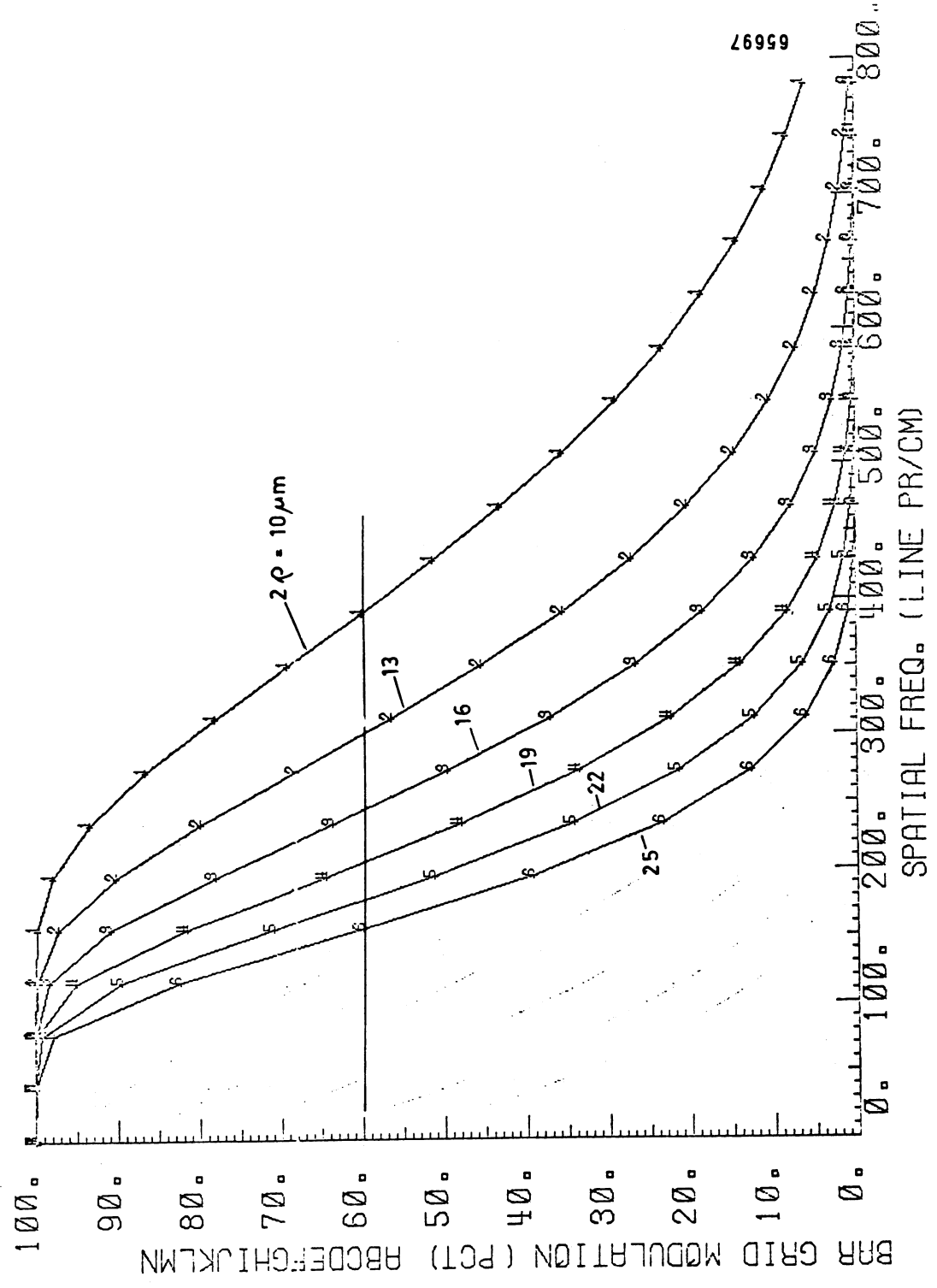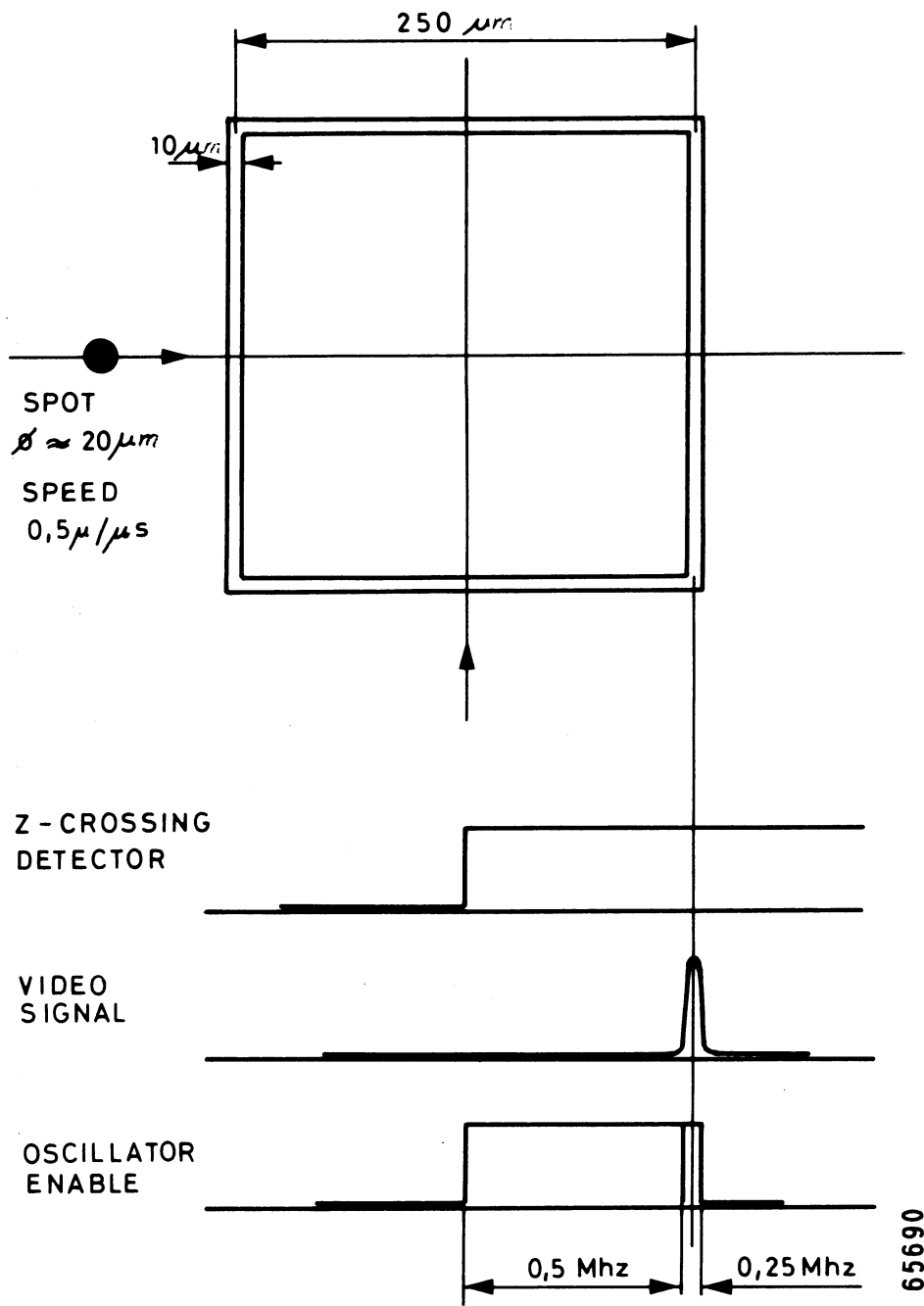
Fig. 8
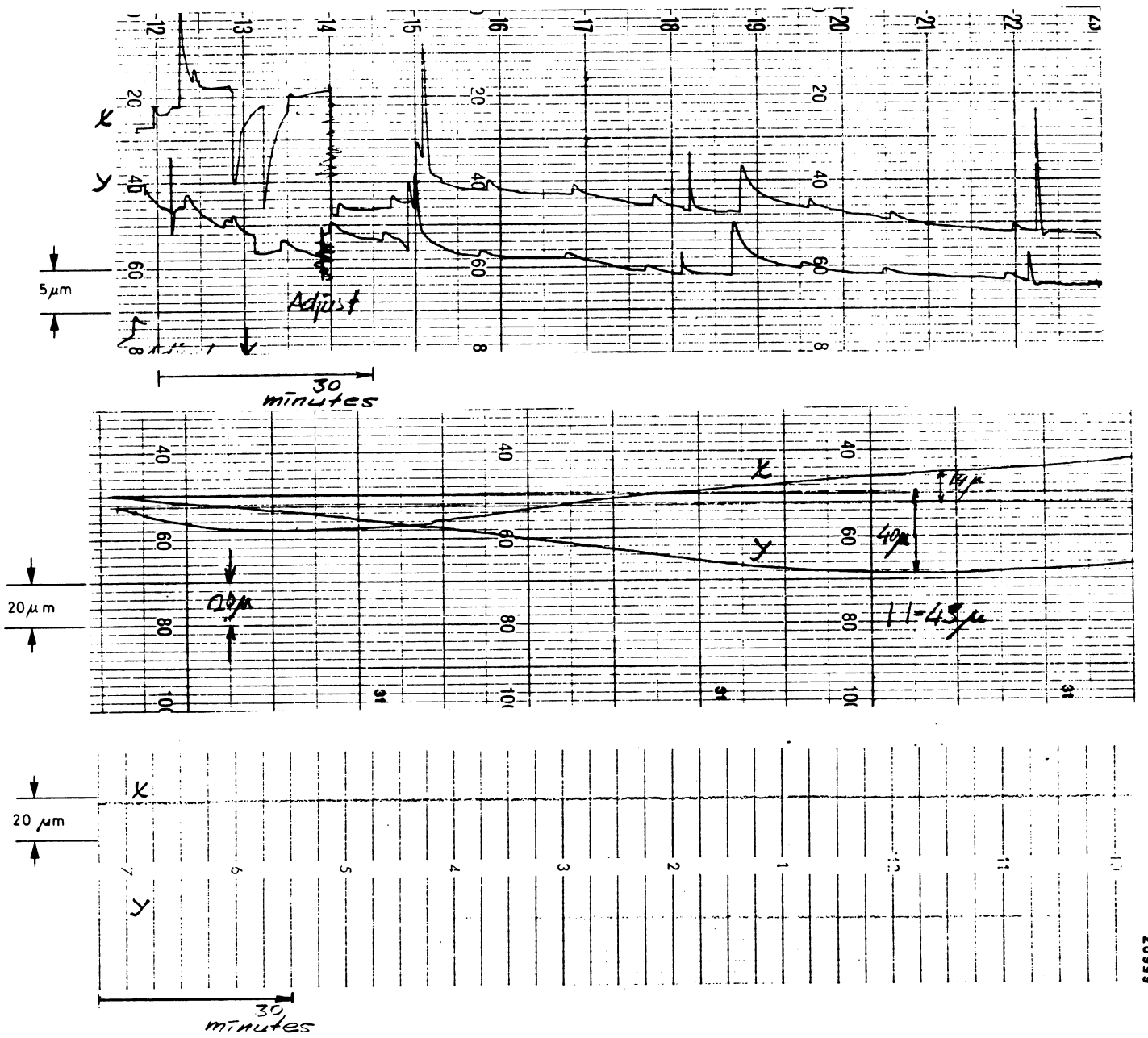
Fig. 9
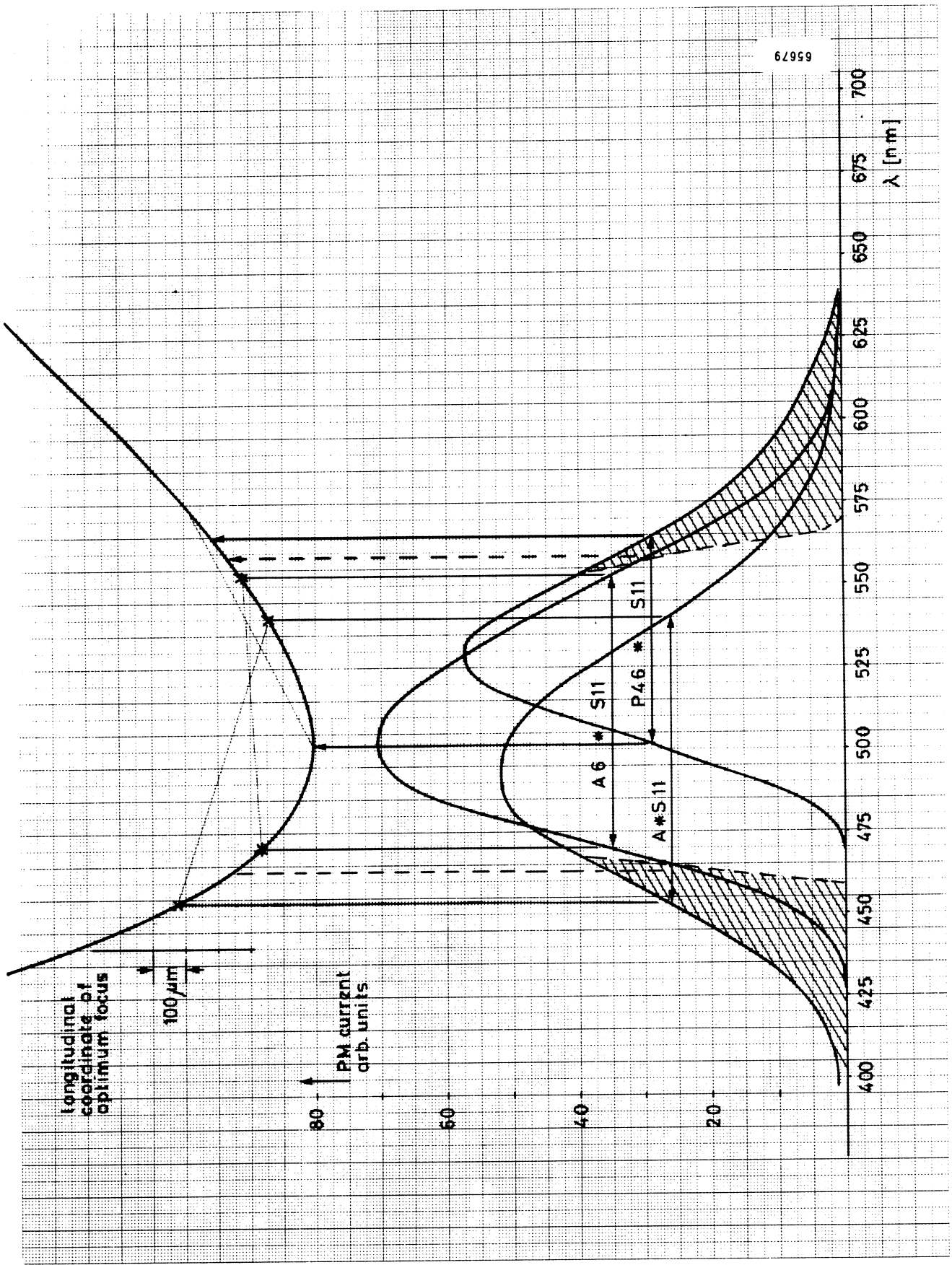
Fig. 10
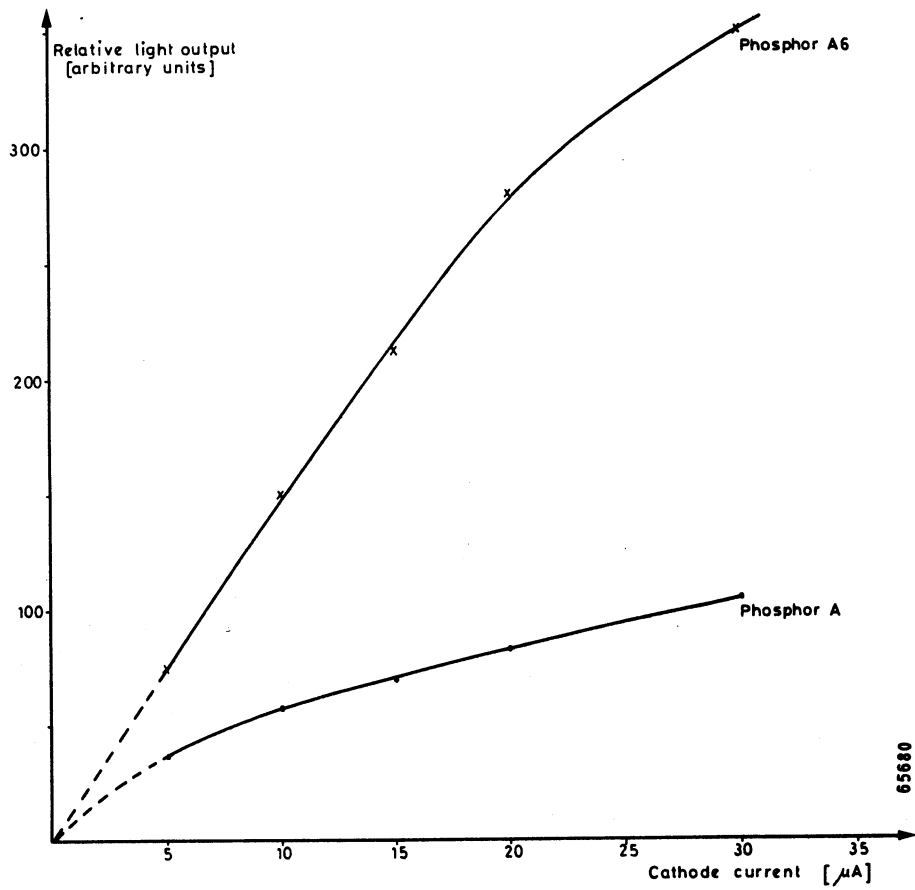
Fig. 11

65681
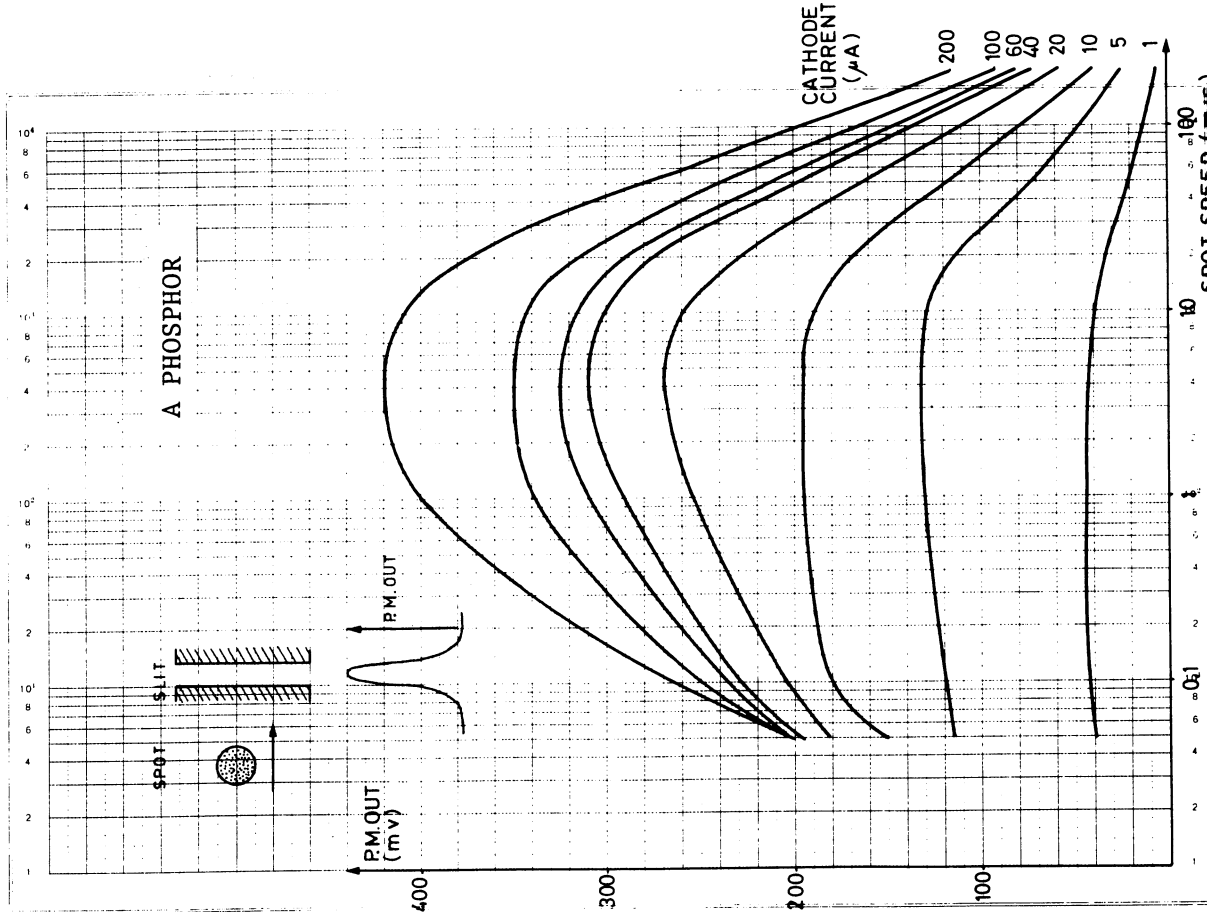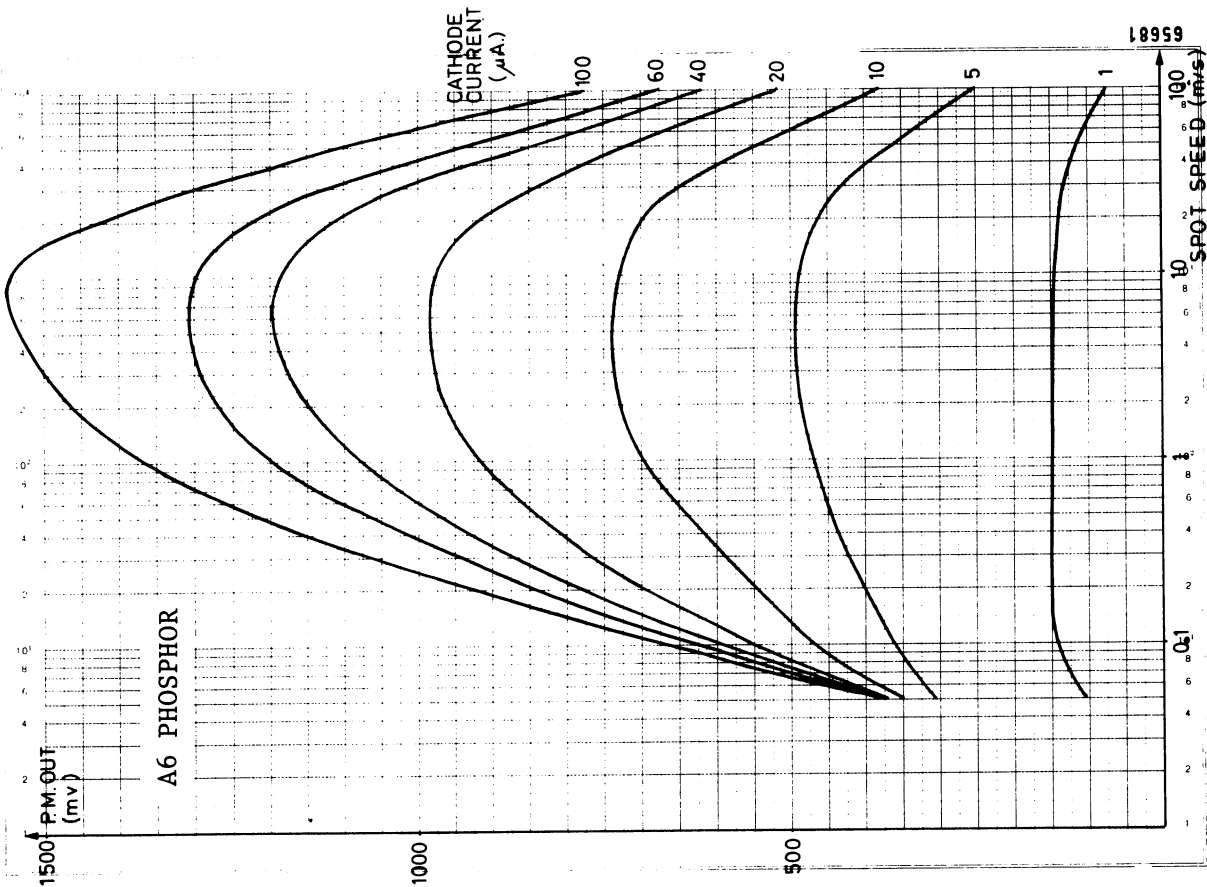
Fig. 12
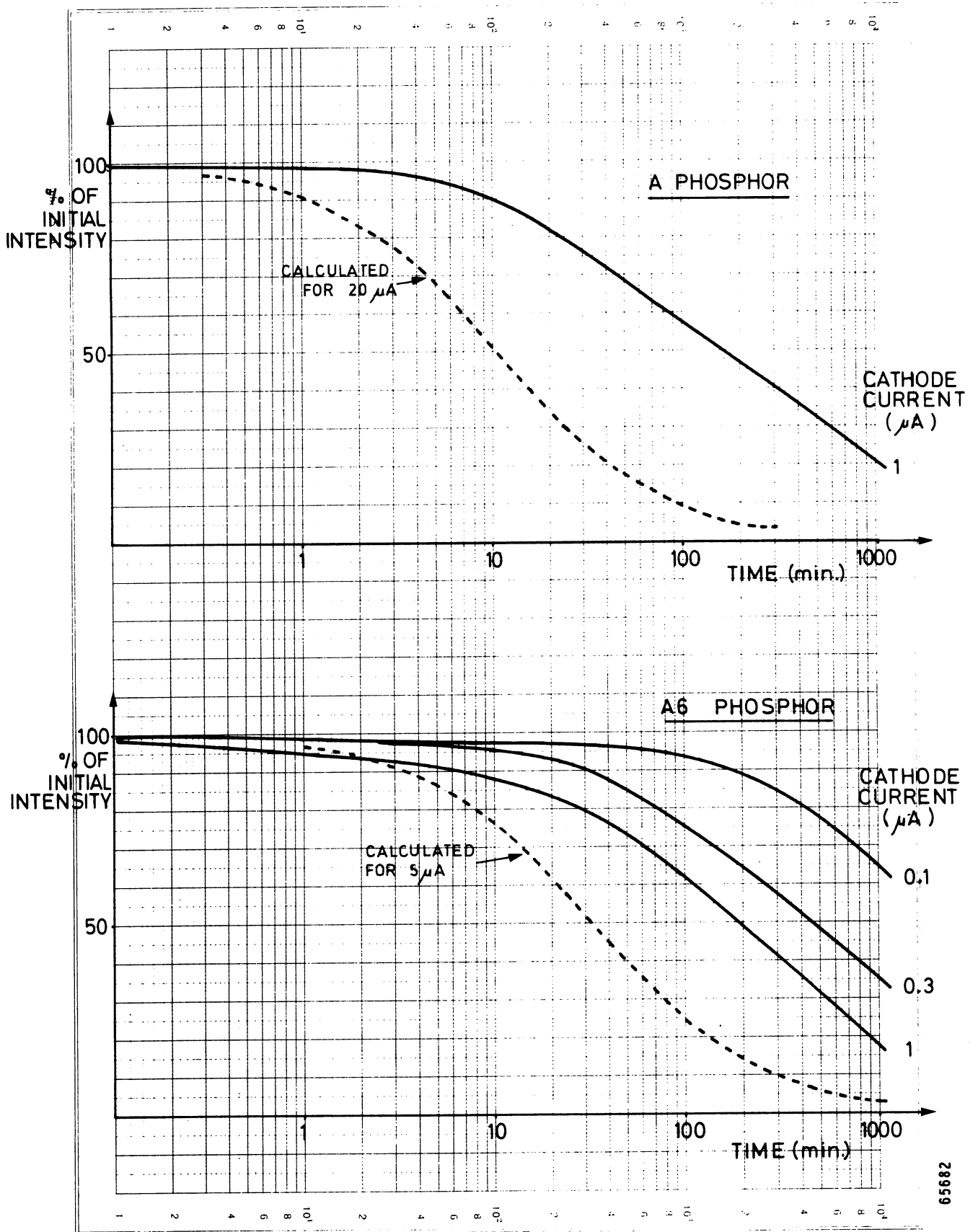
Fig. 13
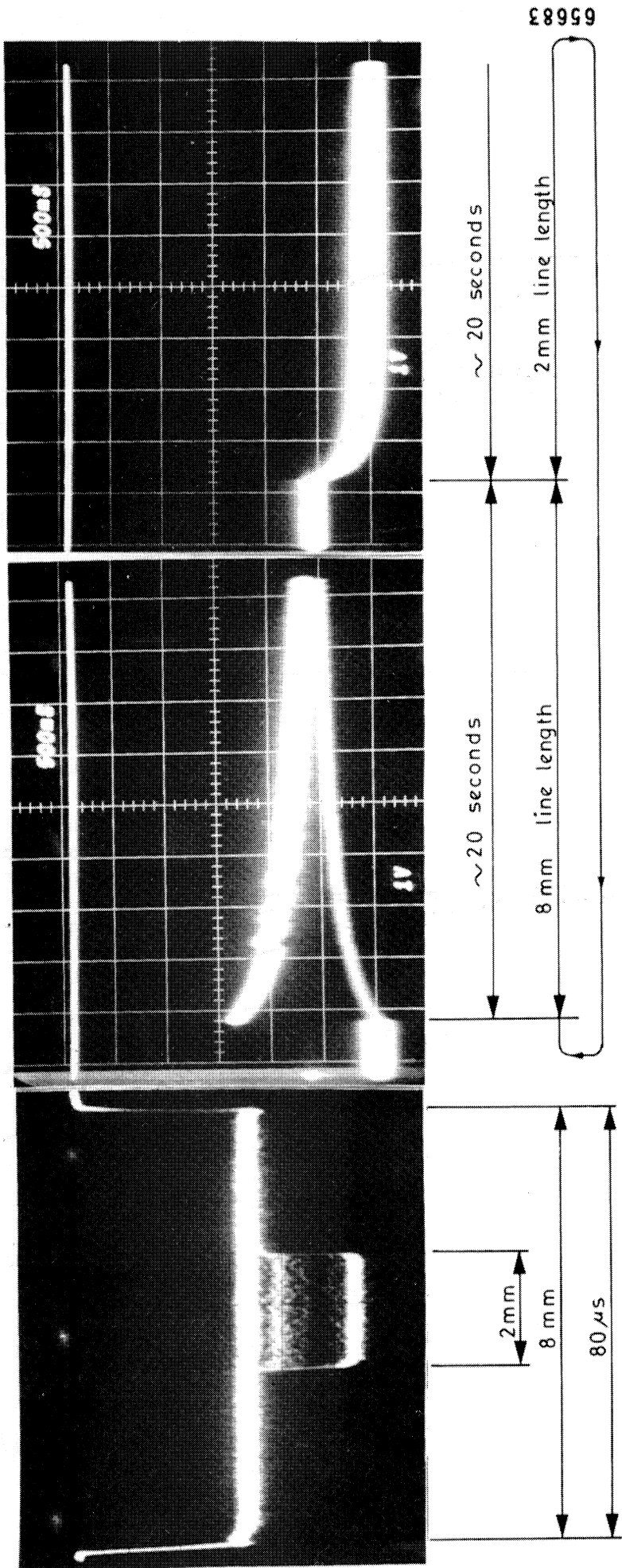
Fig. 14

Optical
magnification

1 : 0,8
(nominal value)

a

100 %
75 %
41 %

1 : 1

b

100 %
72 %
39 %
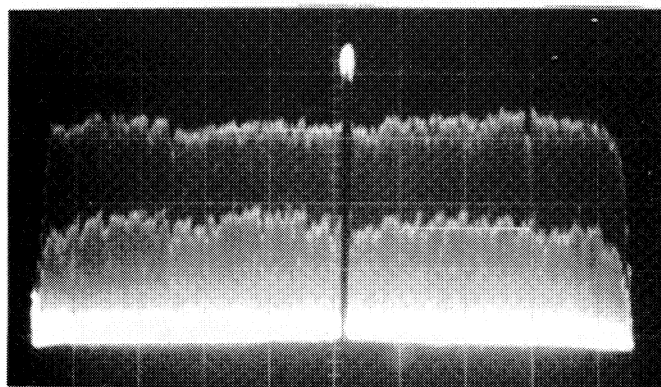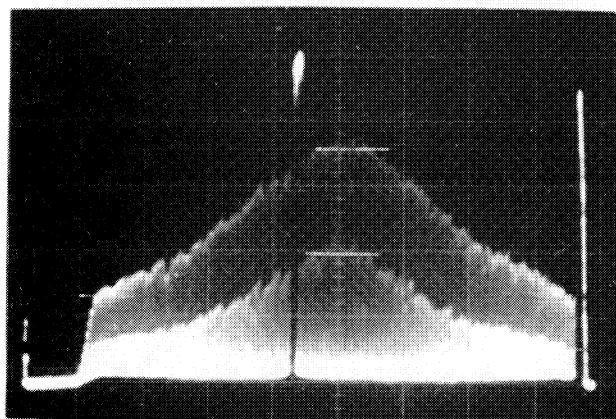
1 : 1,2
(lens reversed)

c
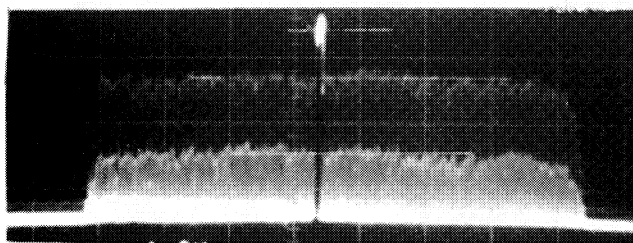
100 %
74 %
33 %

65695

Fig. 15

test grid :

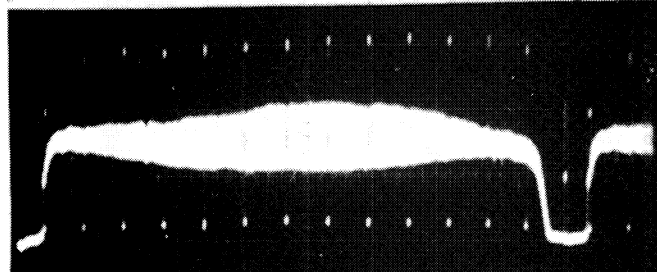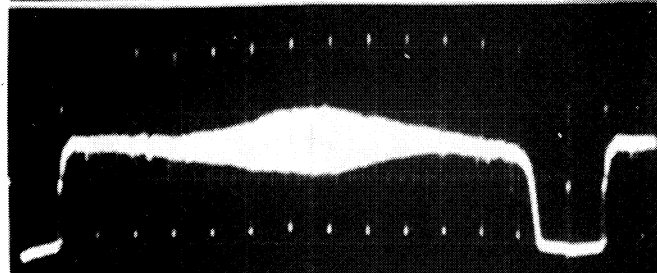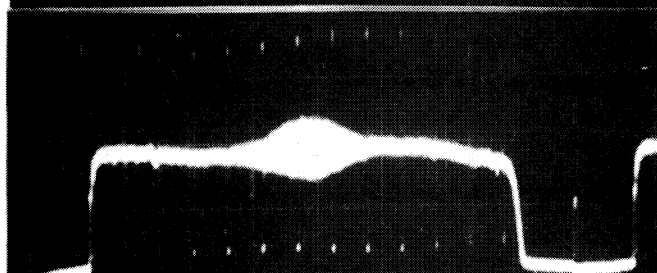30 μm   10 mm
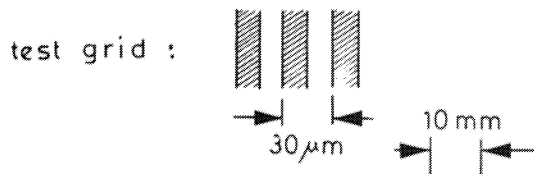
Optical
magnification
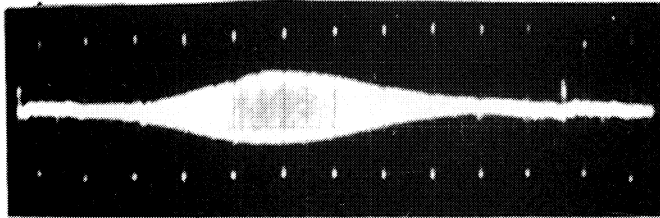
1 : 0,7
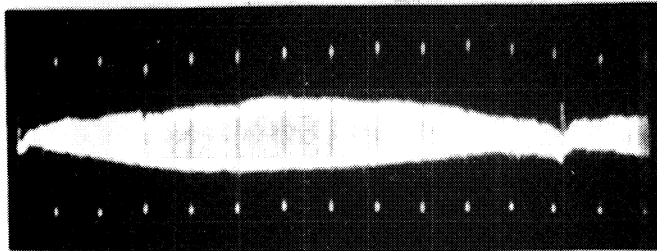
1 : 0,75
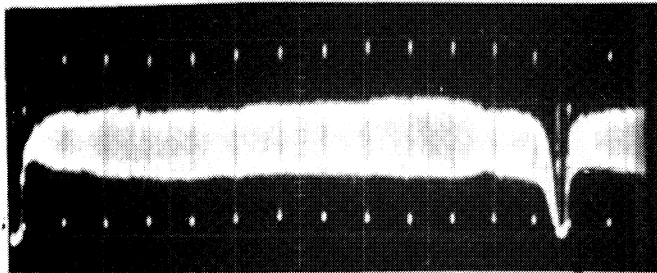
1 : 0,8
(nominal value)

1 : 0,85

1 : 0,9

1 : 1

65696

Fig. 16